Switching in Nanoscale Molecular Junctions due to Contact Reconfiguration

Ornago, Luca; Kamer, Jerry; El Abbassi, Maria; Grozema, Ferdinand C.; Van Der Zant, Herre S.J.

DOI
10.1021/acs.jpcc.2c04370

Publication date
2022

Document Version
Final published version

Published in
Journal of Physical Chemistry C

THE JOURNAL OF PHYSICAL CHEMISTRY C
A JOURNAL OF THE AMERICAN CHEMICAL SOCIETY

pubs.acs.org/JPCC

Article

Switching in Nanoscale Molecular Junctions due to Contact Reconfiguration

Luca Ornago, Jerry Kamer, Maria El Abbassi, Ferdinand C. Grozema, and Herre S.J. van der Zant*

Cite This: https://doi.org/10.1021/acs.jpcc.2c04370

Read Online

ACCESS | Metrics & More | Article Recommendations | Supporting Information

ABSTRACT: Switching effects are key elements in the design and characterization of nanoscale molecular electronics systems. They are used to achieve functionality through the transition between different conducting states. In this study, we analyze the presence of switching events in reference molecular systems, which are not designed to have switching behavior, such as oligo(phenylene ethynylene)s and alkanes, using the mechanically controllable break junction technique. These events can be classified in two groups, depending on whether the breaking trace shows exponential decay or plateau-like features before the switch happens. We argue that the former correspond to junctions forming after rupture of the gold atomic point contact, while the latter can be related to a change in the contact geometry of the junction. These results highlight how a proper choice of anchoring group and careful comparison with reference compounds are essential to understanding the origin of switching in molecular break junctions.

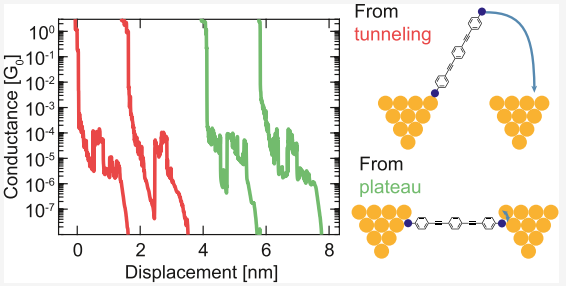

INTRODUCTION

Nanoscale molecular junctions have been investigated for decades in order to use molecules as building blocks in electronic devices.[1] Charge transport properties of such structures are often investigated using break-junction techniques.[2] Among these, stretching-based methods [such as scanning tunneling microscope break junctions (STM-BJ) and mechanically controllable break junctions (MCBJ)] have been widely employed because of the possibility of acquiring large statistical sets of data,[3] which are then used to build one- and two-dimensional conductance histograms. This statistical analysis, however, hides information that can be obtained from individual breaking traces. For instance, spring-like molecules can show mechanosensitivity (i.e., conductance variations as a function of displacement), which get smeared out when averaged in a histogram.[4]

Another class of features that can be hidden by histograms is switching events, that is, sudden changes of current flowing through the junction. Unconventional increases of conductance during stretching have, for example, been linked to deprotonation of the anchoring group in a pyrazolyl-terminated molecule.[5] Another proposed mechanism of switching consists of flipping between conformations in crank-like molecules.[6] As an additional consideration, González et al.[7] analyzed the elongation behavior of an oligo(phenylene ethynylene)s (OPE3) diamine. In this study, they indicate that the presence of traces with switching events is linked to the formation of single-molecule junctions, where the bonding to the gold electrode is broken and reformed multiple times. Instead, traces showing no switching originate from junctions where multiple molecules bridge the nanogap. A more recent study by Chen et al.[8] analyzed the presence of switching events in diamine- and dithiol-terminated alkanes using a novel technique. They found good agreement with previously proposed explanations of multiple conductance states in alkanes.[9]

Thus, the presence of switching events is a frequent feature in STM-BJ and MCBJ measurements. It is observed both in conjugated and non-conjugated molecules, in molecules whose backbone is changing upon external stimuli, and it can also be related to the nature of the anchoring group. A comparative study that systematically analyzes the effect of both the molecular backbone and the anchoring group would help shed light on this phenomenon.

For this reason, we analyze the presence of switching events in OPE3s derivatives and in two alkanes (hexane and octane). Both systems are well-studied benchmark molecules in molecular electronics, the former having a rigid conjugated backbone,[10−15] the latter having a flexible, non-conjugated one.[9,16−21] Additionally, we consider different anchoring groups for each molecule. For OPE3, we use amino ($-NH_2$), pyridine (−Pyr), thiomethyl (−SMe), and acetate-protected thiol (−SAc). For alkanes, we opt for diamino ($-NH_2$) and dithiol (−SH) termination. This selection allows

Received: June 23, 2022
Revised: October 11, 2022

one to explore strong covalent binding to the electrodes (−SAc and −SH), as well as the weaker dative one (−NH_2, −Pyr, and −SMe). The use of these backbones and anchors will constitute a solid foundation for future studies on switching in metal-molecule-metal junctions.

METHODS

OPE3-SAc, hexanedithiol, hexanediamine, octanedithiol, and octanediamine were purchased from Sigma-Aldrich and used without further purification. OPE3-NH_2, OPE3-Pyr, and OPE3-SMe were obtained, as described in ref 15. The chemical structure of the compounds analyzed in this study is shown in Figure 1. The conductance of the molecules was characterized using the MCBJ technique. Details of the method can be found in previous works.[22] Prior to the measurement, the devices were characterized without molecules to assure their cleanliness (see Supporting Information, Figure S2). Then, about 5 μL of the molecular solution was drop-cast on the device. Unless otherwise stated, the OPE3-based solutions had a concentration of 0.1 mM, while alkane-based solutions were 1 μM, both in dichloromethane (Sigma-Aldrich). After full solvent evaporation, thousands of consecutive breaking traces were recorded on each device, using a constant bias voltage of 0.1 V and actuation speeds of either 50 or 200 V s^{-1}. A detailed overview of the measurements can be found in the Supporting Information, Section S2.

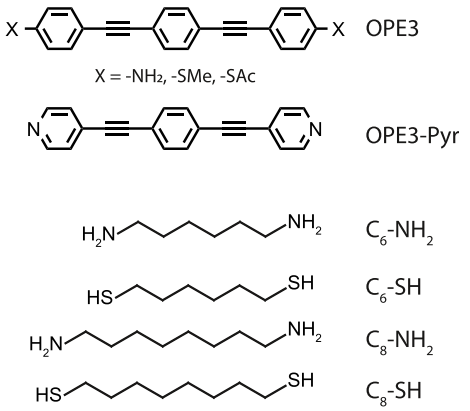

Figure 1. Chemical structures of the compounds analyzed in this study.

RESULTS AND DISCUSSION

Although MCBJ measurements consist of individual conductance−displacement curves, the first step in the analysis is to collect all the measured traces in histograms. In this way, it is possible to observe the most prominent features in the measurement. As an example, the two-dimensional conductance versus electrode displacement histogram of OPE3-NH_2 is shown in Figure 2a and displays two plateaus, with corresponding peaks in the one-dimensional histogram, independently fitted to separate log−normal distributions (shaded blue and green areas in Figure 2a): a high-conductance one at $4.5 \times 10^{-5} G_0$ and a low-conductance one at $1.0 \times 10^{-6} G_0$. Here, $G_0 = \frac{2e^2}{h} \approx 77.5\ \mu S$ is the conductance quantum, where e is the electron charge and h is

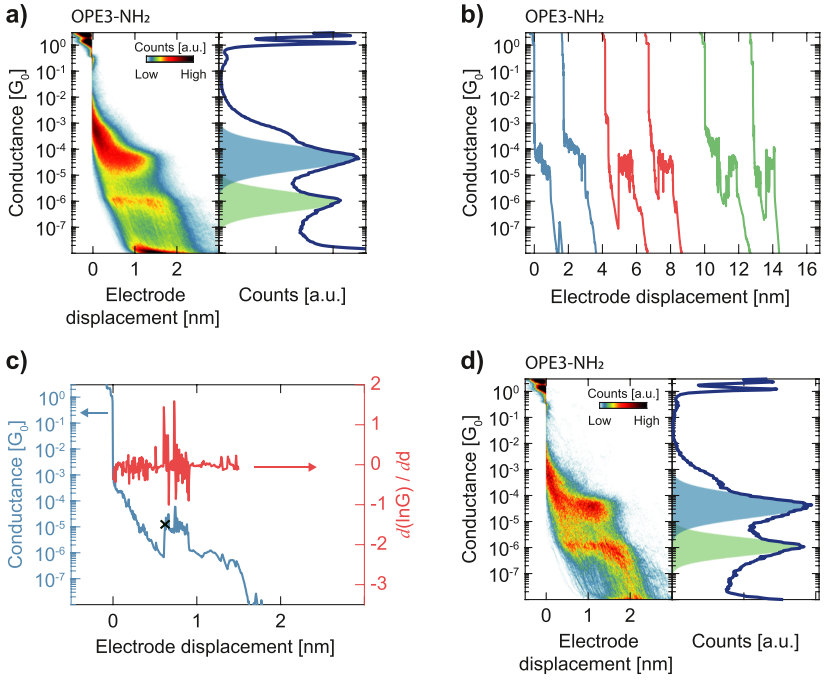

Figure 2. (a) Two-dimensional conductance−displacement histogram (left) and the corresponding one-dimensional conductance histogram (right) of OPE3-NH_2. The light blue and green shaded areas are the fits to the high- and low-conductance plateau, respectively. (b) Examples of individual traces showing different behaviors: stable plateau (blue), switching between tunneling and a molecular plateau (red), and switching between two molecular plateaus (green). Curves are displaced in the x-direction for better visibility. (c) Illustration of the classification procedure used to separate traces containing switches: in blue, an example of a molecular trace showing a switch, and in red, the corresponding derivative used to identify jumps. The black cross identifies the average conductance identified after the jump. (d) Two-dimensional conductance−displacement histogram (left) and one-dimensional conductance histogram (right) constructed using only traces that show jumps obtained from the same OPE3-NH_2 measurement shown in panel (a).

https://doi.org/10.1021/acs.jpcc.2c04370
J. Phys. Chem. C XXXX, XXX, XXX−XXX

the Planck's constant. The presence of multiple plateau-like features in MCBJ measurements of OPE3 has been widely discussed in the literature. Plateaus with conductance around $10^{-6}G_0$ are attributed either to the presence of π-stacked dimers or to presence of multiple binding configurations.[12,14] Notice that the measurement also shows a peak at higher conductance than the $4.5 \times 10^{-5}G_0$ peak. Plateaus at conductance higher than the prevalent one have been observed before for OPE3-SAc.[23,24] In particular, its intensity correlates with the molecular yield, that is, the number of traces showing a plateau with respect to the total number of traces and it can be observed in OPE3 with different anchoring groups, albeit with varying intensity across measurements (Figures S3–S7). Its origin is at present not fully understood; a detailed analysis of this aspect lies outside the scope of this work. When inspecting individual traces, most show a continuous plateau until the junction ruptures (blue curves in Figure 2b), but not all of them: breaking traces can exhibit switching either after an exponential decay (red curves in Figure 2b) or after a plateau with a different conductance (green curves in Figure 2b). The same behaviors have been reported by others.[5,7,21]

In order to quantify the presence of such switching events, we developed an algorithm that works as follows: the derivative of the conductance is computed in a defined region of interest, and its peaks were identified as possible locations for switching events. Going in order of decreasing peak height, each peak was further analyzed by checking the difference in conductance before and after the switch. This was done to avoid noise spikes being detected as switches in conductance. If the difference clears the set threshold, the trace is marked as having a switch, and the displacement at which the peak appears is saved. An example of how the algorithm operates is shown in Figure 2c. For further details on the algorithm, we refer to Supporting Information, Section S1. Notice that we restrict this analysis to the first switch found in each trace. Additionally, in some cases, the conductance switches downward after the high-conductance plateau ends. We exclude this event from our analysis because first it is well discussed in the literature[9,14] and second, we want to focus on the cases in which the conductance is able to switch back to a higher value.

Focusing first on the OPE3-NH_2 measurement shown in Figure 2a, the algorithm found switching events in 22% of molecular traces. Figure 2d displays the histograms obtained using only switching traces. The high-conductance plateau built from those has the most probable conductance of $3.9 \times 10^{-5}G_0$. Instead, when considering only traces showing no switch the most probable conductance is $4.5 \times 10^{-5}G_0$, higher than the one containing the switching traces. This trend is consistent across measurements (see Supporting Information, Table S2) and with the previous observations by González et al.[7]

Effect of the Anchoring Group. Switching events can be detected across the OPE3s with different anchoring groups, as shown in Figure 3. OPE3-SMe presents a similar behavior to OPE3-NH_2, meaning that the 2D-histograms built from switching traces are similar to the ones built from raw data. OPE3-Pyr exhibits a different behavior: the conductance switch happens after an exponential decay, at a well-defined displacement. This is emphasized when considering the master trace, that is, the trace built using the most probable conductance at each displacement in the 2D-histogram (black lines in Figure 3). The yield of molecular traces with

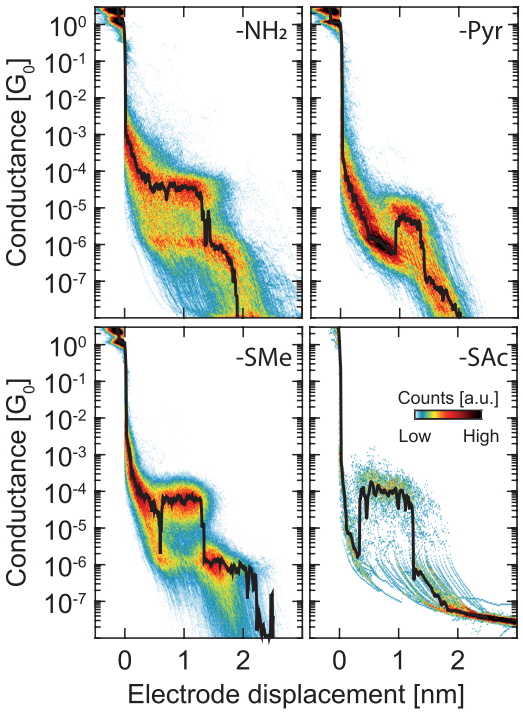

Figure 3. 2D conductance–displacement histograms of OPE3-NH_2, OPE3-Pyr, OPE3-SMe, and OPE3-SAc built using only traces that show switching. The master trace (black line) is superimposed on the corresponding histogram. The yield of switching events is 27% for OPE3-NH_2, 41% for OPE3-Pyr, 16% for OPE3-SMe, and 3% for OPE3-SAc. These values are obtained as the average of the measurements at 50 V s^{-1} reported in the Supporting Information, Tables S1, S3, and S5.

respect to the number of molecular traces is similar among different anchoring groups, with the exception of –SAc anchoring. The latter has a drastically lower probability of showing switching events (Supporting Information, Tables S1, S3, and S5). The origin of this difference is likely the stronger covalent bonds formed by the thiol groups upon deprotection.[15,25] Additionally, we observe a large variation of switching probabilities across different measurements of the same molecule. For example, for OPE3-NH_2 this probability ranges from 13 to 52% of molecular traces (Table S1).

Traces without switching show a plateau with a higher most-probable conductance than the corresponding one in switching traces: the peak position in the one-dimensional-conductance histogram is 24% higher for OPE3-Pyr, 30% for OPE3-NH_2, 42% for OPE3-SAc, and 59% for OPE3-SMe (Supporting Information, Tables S2, S4, and S6). Notice that traces without switching usually have comparable conductance to the raw data. This can be explained by considering that if a trace is switching, it will have fewer counts at the plateau conductance. Hence, in the raw data, the most-probable conductance value will be mostly determined by non-switching traces. These results are compatible with the work by González et al.[7] Here, we show that the trend holds for OPE3 with several anchoring groups.

Types of Switching Events. It is possible to distinguish between two types of switching events, as hinted in the previous section: the ones occurring after a steep exponential decay ("tunneling" switch), and the ones that occur between two different plateaus ("plateau" switch). To better characterize the presence of these types of events in the measurements,

https://doi.org/10.1021/acs.jpcc.2c04370
J. Phys. Chem. C XXXX, XXX, XXX–XXX

we further filter the switching traces by considering the slope of the trace before the switch. In a measurement showing no molecular plateaus, traces with a slope greater than −3 decades nm^{-1} are not expected (see Supporting Information, Section S3). Thus, if a molecular trace shows a slope smaller than this value before switching, it is labeled a tunneling switch. If the slope is greater, it is considered to be from a plateau.

This procedure allows one to track the presence of both types of events in OPE3-SMe (Figure 4a, Supporting Information, Table S10) and OPE3-NH_2 (Supporting Information, Table S9). Tunneling switches occur after a defined displacement, which is reflected by the isolated cloud of counts between 0.8 and 1.4 nm in Figure 4a (left). This type of behavior closely resembles that of OPE3-Pyr (Figure 3). On the contrary, the histograms built with plateau switches do not show this cloud-like feature. This hints an interesting behavior: the junctions first show the slope typical of empty traces. Then, they switch to the molecular feature at a consistent displacement. Because of this, the area in the 2D-histogram corresponding to the plateau appears isolated from the rest.

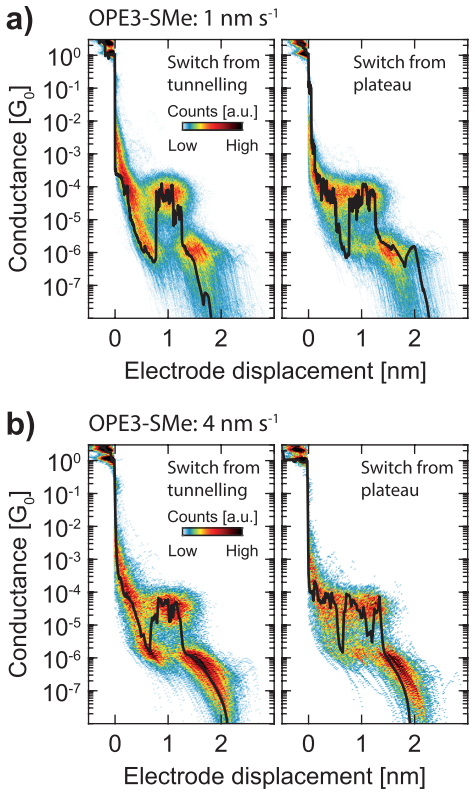

Figure 4. 2D conductance−displacement histograms of switching traces in OPE3-SMe at (a) 1 and (b) 4 nm s^{-1}, divided in traces that show switching starting from tunneling (left) and ones that show switching starting from a plateau (right). An example trace (black line) of each kind of switching event is superimposed to the corresponding histogram.

Increasing the breaking speed from 1 to 4 nm s^{-1} does not influence the presence of either type of switching event nor does it change the displacement at which the switch happens in the tunneling events (see Figure 4b). This implies that, in the explored stretching rate range, tunneling switches are not related to time-dependent phenomena, such as thermal adsorption/desorption of the molecule from the electrode. We note that according to previous reports[26] these effects start to be dominant only at stretching rates below 1 nm s^{-1}, or that they are not relevant at all.[7]

A possible explanation for the tunneling switching is that these are due to a junction forming while separating the electrodes, with molecules initially anchored to only one, as illustrated in Figure S17. Because in the experiments the switch occurs at a well-defined displacement, one can conceive that after this critical displacement is reached, the dangling side of the molecule "snaps" to connect to the other electrode. In this picture, the threshold should correspond to the minimum distance between the free anchoring group of the molecule and the apex of the electrode (i.e., the site at which the driving force for binding is the largest). This is, in principle, a similar mechanism to what drives atomic force microscopy or STM tips functionalization procedures.[27] However, this explanation is in contrast with a previously reported study in STM-BJ,[28] where it is found that junction formation happens before the rupture of the gold contact. Although, it is important to highlight that in this study the measurements were performed in solution. Additionally, the tip−substrate geometry of the STM setup is different from the MCBJ lithographically defined nanowire. These differences could be at the origin of the contrasting results.

Plateau switching suggests that the junction is changing between different configurations. Because there are no intrinsic molecular switching mechanisms in the rigid OPE3 backbone, the most likely explanation is that the contact configuration with the gold surface is changing, similarly suggested by Kaliginedi et al.[14] We therefore examined the length of the segments in which the junction remains in the low-conductance state, as described in Supporting Information, Section S3.1. The resulting histograms are shown in Supporting Information, Figures S12 and S15. We find that OPE3-NH_2 and OPE3-SMe have a prominent narrow peak at lengths of 0.1 ± 0.02 and 0.1 ± 0.04 nm, respectively. In addition, we also observe broader peaks at 0.3 ± 0.06 and 0.3 ± 0.04 nm, respectively (Supporting Information, Tables S12 and S13). As a first estimate, these values can be compared to the distance between different sites on the gold surface. Considering an Au(111) surface with an interatomic distance of 0.2884 nm,[29] there are three types of adsorption sites: on-top, bridge (in-between two gold atoms), and close packed (surrounded by 3 atoms).[30] The distance that a molecule needs to cover to move from an on-top site to a bridge one is 0.14 or 0.25 nm depending on the direction, while moving to a close packed site requires 0.17 nm.

An alternative explanation for plateau switching is the disconnection (and subsequent reconnection) of one side of a molecule in a π-stacked dimer, as illustrated in Supporting Information, Figure S17. We cannot exclude this mechanism; however, it is unlikely that an event that causes the rupture of the gold molecule contact would still preserve the intermolecular geometry. Theoretical studies combining molecular dynamics with transport calculations are needed to reveal the details of the junction evolution.

Switching in Alkanes Molecular Junctions. We also analyzed a set of MCBJ measurements on alkanes previously published by our group.[21] Alkanes show a much smaller difference between the conductance states before and after the switch compared to OPE3. This is evident from the 2D-histograms shown in Supporting Information, Section S2.2 (compare, e.g., the histograms of OPE3-NH_2 in Figure S3 with the ones of C6 in Figure S8 and C8 in Figure S9). The other

https://doi.org/10.1021/acs.jpcc.2c04370
J. Phys. Chem. C XXXX, XXX, XXX−XXX

striking difference between alkanes and OPE3 is that in the former the amount of switching events for the (−SH)-terminated compounds is higher than for ($-NH_2$) (Table S7). However, alkanediamines show much clearer switching behavior in their histograms (Figures S8 and S9). This can have different explanations. First, dithiol−alkanes were measured without the use of a deprotecting agent. This could lead to the presence of weaker bonds to the gold surface.[25] However, this is unlikely to be the only cause. In fact, when measuring OPE3-SAc without deprotecting agent, we find a slight increase of switching events (Table S5), but the value is not close to the one observed for OPE3-NH_2. Another possible explanation stems from the several junction configurations that alkanes are expected to form when bound to gold, such as gauche conformations,[9] or chaining of multiple units.[31] This leads to more mechanisms through which the conductance can switch, thus increasing the yield of such events.

Additionally, the analyzed alkane measurements show mostly tunneling type switching, although the classification is less clear than for OPE3s (see Supporting Information, Section S3). The origin of this observation could be purely technical: because hexane and octane are relatively short molecules, it is possible that they do not spend enough time in the junction to spontaneously switch between different states, especially considering the measurement speed at which these measurements were carried out. It would be interesting to repeat such measurements with a low measurement speed to see if the presence of plateau switches increases.

Lastly, we analyzed the length of the low-conductance segments for plateau switches in alkanes. We find that they show a distribution with one peak at 0.2 nm for all of them (only C6-SH showing a clear additional peak at 0.1 nm, see Supporting Information, Figure S16 and Table S14), differently from OPE3s. In terms of displacement, this can still be explained by the switch between different contact sites on the gold surface. However, gauche defects in alkanes are also expected to happen in a similar displacement range,[19] making it difficult to disentangle the two phenomena.

CONCLUSIONS

In conclusion, we identify the presence of switching events in MCBJ measurements of OPE3, hexane, and octane, having different anchoring groups. However, in the case of OPE3-SAc, the amount of switching events can be considered negligible. Additionally, we identify two types of switching. "Tunneling" switching happens after an exponential decay of conductance typical of empty traces, which suggests the possibility of junction formation after rupture of the gold bridge. "Plateau" switching happens while the trace is already showing a clear molecular plateau right after breaking of the gold contact. These can be related to the junction changing its configuration during the measurement, either to a junction with weaker coupling to the electrodes, or to a π-stacked dimer. This study highlights the necessity to carefully consider the anchoring groups when studying abrupt conductance changes in molecular switches. Acetate-protected thiol (−SAc) is confirmed as a stable anchoring option showing no relevant amount of switching. Otherwise, coexistence of contact-dependent mechanisms and chemically introduced backbone-related mechanisms thus requires either careful selection of anchoring groups or one-to-one comparison to reference compounds. Our study gives a perspective in what can be expected from some of the most studied reference molecules.

ASSOCIATED CONTENT

Supporting Information

The Supporting Information is available free of charge at https://pubs.acs.org/doi/10.1021/acs.jpcc.2c04370.

Details on measurements and analysis, example trace, overview of the measurements, conductance of the measurements, two-dimensional conductance−displacement, histogram, results of the classification, fitted length values, and schematic illustration (PDF)

The MCBJ measurements data is available free of charge at https://doi.org/10.4121/20465781.

AUTHOR INFORMATION

Corresponding Author

Herre S.J. van der Zant − *Kavli Institute of Nanoscience, Delft University of Technology, 2628 CJ Delft, The Netherlands;* orcid.org/0000-0002-5385-0282; Email: H.S.J.vanderZant@tudelft.nl

Authors

Luca Ornago − *Kavli Institute of Nanoscience, Delft University of Technology, 2628 CJ Delft, The Netherlands;* orcid.org/0000-0001-5293-2887

Jerry Kamer − *Kavli Institute of Nanoscience, Delft University of Technology, 2628 CJ Delft, The Netherlands*

Maria El Abbassi − *Kavli Institute of Nanoscience, Delft University of Technology, 2628 CJ Delft, The Netherlands;* orcid.org/0000-0001-5177-6528

Ferdinand C. Grozema − *Department of Chemical Engineering, Faculty of Applied Sciences, Delft University of Technology, 2629 HZ Delft, The Netherlands;* orcid.org/0000-0002-4375-799X

Complete contact information is available at: https://pubs.acs.org/10.1021/acs.jpcc.2c04370

Notes

The authors declare no competing financial interest.

ACKNOWLEDGMENTS

This study was partially funded by the FET open project 394 QuIET (no. 767187). The Device Fabrication was performed at the Kavli Nanolab at Delft University of Technology.

REFERENCES

(1) Xiang, D.; Wang, X.; Jia, C.; Lee, T.; Guo, X. Molecular-scale electronics: from concept to function. *Chem. Rev.* **2016**, *116*, 4318−4440.

(2) Gehring, P.; Thijssen, J. M.; van der Zant, H. S. J. Single-molecule quantum-transport phenomena in break junctions. *Nat. Rev. Phys.* **2019**, *1*, 381−396.

(3) Xiang, D.; Jeong, H.; Lee, T.; Mayer, D.; Xiang, D.; Jeong, H.; Lee, T.; Mayer, D. Mechanically controllable break junctions for molecular electronics. *Adv. Mater.* **2013**, *25*, 4845−4867.

(4) Stefani, D.; Weiland, K. J.; Skripnik, M.; Hsu, C.; Perrin, M. L.; Mayor, M.; Pauly, F.; van der Zant, H. S. J. Large Conductance Variations in a Mechanosensitive Single-Molecule Junction. *Nano Lett.* **2018**, *18*, 5981−5988.

(5) Herrer, I. L.; Ismael, A. K.; Milán, D. C.; Vezzoli, A.; Martín, S.; González-Orive, A.; Grace, I.; Lambert, C.; Serrano, J. L.; Nichols, R. J.; et al. Unconventional single-molecule conductance behavior for a

new heterocyclic anchoring group: pyrazolyl. *J. Phys. Chem. Lett.* **2018**, *9*, 5364−5372.
(6) Qu, K.; Duan, P.; Wang, J.-Y.; Zhang, B.; Zhang, Q.-C.; Hong, W.; Chen, Z.-N. Capturing the rotation of one molecular crank by single-molecule conductance. *Nano Lett.* **2021**, *21*, 9729−9735.
(7) González, M. T.; Díaz, A.; Leary, E.; García, R.; Herranz, M. Á.; Rubio-Bollinger, G.; Martín, N.; Agraït, N. Stability of single- and few-molecule junctions of conjugated diamines. *J. Am. Chem. Soc.* **2013**, *135*, 5420−5426.
(8) Chen, H.; Li, Y.; Chang, S. Hybrid molecular-junction mapping technique for simultaneous measurements of single-molecule electronic conductance and its corresponding binding geometry in a tunneling junction. *Anal. Chem.* **2020**, *92*, 6423−6429.
(9) Li, C.; Pobelov, I.; Wandlowski, T.; Bagrets, A.; Arnold, A.; Evers, F. Charge transport in single Au |alkanedithiol| Au junctions: Coordination geometries and conformational degrees of freedom. *J. Am. Chem. Soc.* **2008**, *130*, 318−326.
(10) Mayor, M.; Weber, H. B.; Reichert, J.; Elbing, M.; von Hänisch, C.; Beckmann, D.; Fischer, M. Electric current through a molecular rod - relevance of the position of the anchor groups. *Angew. Chem., Int. Ed.* **2003**, *42*, 5834−5838.
(11) Huber, R.; González, M. T.; Wu, S.; Langer, M.; Grunder, S.; Horhoiu, V.; Mayor, M.; Bryce, M. R.; Wang, C.; Jitchati, R.; et al. Electrical conductance of conjugated oligomers at the single molecule level. *J. Am. Chem. Soc.* **2008**, *130*, 1080−1084.
(12) Wu, S.; González, M. T.; Huber, R.; Grunder, S.; Mayor, M.; Schönenberger, C.; Calame, M. Molecular junctions based on aromatic coupling. *Nat. Nanotechnol.* **2008**, *3*, 569−574.
(13) González, M. T.; Leary, E.; García, R.; Verma, P.; Herranz, M. Á.; Rubio-Bollinger, G.; Martín, N.; Agraït, N. Break-junction experiments on acetyl-protected conjugated dithiols under different environmental conditions. *J. Phys. Chem. C* **2011**, *115*, 17973−17978.
(14) Kaliginedi, V.; Moreno-García, P.; Valkenier, H.; Hong, W.; García-Suárez, V. M.; Buiter, P.; Otten, J. L.; Hummelen, J. C.; Lambert, C. J.; Wandlowski, T. Correlations between molecular structure and single-junction conductance: A case study with oligo(phenylene-ethynylene)-type wires. *J. Am. Chem. Soc.* **2012**, *134*, 5262−5275.
(15) Frisenda, R.; Tarkuç, S.; Galán, E.; Perrin, M. L.; Eelkema, R.; Grozema, F. C.; van der Zant, H. S. J. Electrical properties and mechanical stability of anchoring groups for single-molecule electronics. *Beilstein J. Nanotechnol.* **2015**, *6*, 1558−1567.
(16) Chen, F.; Li, X.; Hihath, J.; Huang, Z.; Tao, N. Effect of anchoring groups on single-molecule conductance: Comparative study of thiol-, amine-, and carboxylic-acid-terminated molecules. *J. Am. Chem. Soc.* **2006**, *128*, 15874−15881.
(17) Venkataraman, L.; Klare, J. E.; Tam, I. W.; Nuckolls, C.; Hybertsen, M. S.; Steigerwald, M. L. Single-molecule circuits with well-defined molecular conductance. *Nano Lett.* **2006**, *6*, 458−462.
(18) Park, Y. S.; Whalley, A. C.; Kamenetska, M.; Steigerwald, M. L.; Hybertsen, M. S.; Nuckolls, C.; Venkataraman, L. Contact chemistry and single-molecule conductance: A comparison of phosphines, methyl sulfides, and amines. *J. Am. Chem. Soc.* **2007**, *129*, 15768−15769.
(19) Paulsson, M.; Krag, C.; Frederiksen, T.; Brandbyge, M. Conductance of alkanedithiol single-molecule junctions: A molecular dynamics study. *Nano Lett.* **2009**, *9*, 117−121.
(20) Li, Z.; Mejía, L.; Marrs, J.; Jeong, H.; Hihath, J.; Franco, I. Understanding the conductance dispersion of single-molecule junctions. *J. Phys. Chem. C* **2021**, *125*, 3406−3414.
(21) van Veen, F. H.; Ornago, L.; van der Zant, H. S. J.; El Abbassi, M. Benchmark study of alkane molecular chains. *J. Phys. Chem. C* **2022**, *126*, 8801−8806.
(22) Martin, C. A.; Smit, R. H. M.; van Egmond, R.; van der Zant, H. S. J.; van Ruitenbeek, J. M. A versatile low-temperature setup for the electrical characterization of single-molecule junctions. *Rev. Sci. Instrum.* **2011**, *82*, 53907.
(23) Cabosart, D.; El Abbassi, M.; Stefani, D.; Frisenda, R.; Calame, M.; van der Zant, H. S. J.; Perrin, M. L. A reference-free clustering method for the analysis of molecular break-junction measurements. *Appl. Phys. Lett.* **2019**, *114*, 143102.
(24) El Abbassi, M.; Overbeck, J.; Braun, O.; Calame, M.; van der Zant, H. S. J.; Perrin, M. L. Benchmark and application of unsupervised classification approaches for univariate data. *Commun. Phys.* **2021**, *4*, 1−9.
(25) Valkenier, H.; Huisman, E. H.; van Hal, P. A.; de Leeuw, D. M.; Chiechi, R. C.; Hummelen, J. C. Formation of high-quality self-assembled monolayers of conjugated dithiols on gold: Base matters. *J. Am. Chem. Soc.* **2011**, *133*, 4930−4939.
(26) Tsutsui, M.; Shoji, K.; Morimoto, K.; Taniguchi, M.; Kawai, T. Thermodynamic stability of single molecule junctions. *Appl. Phys. Lett.* **2008**, *92*, 223110.
(27) Bartels, L.; Meyer, G.; Rieder, K.-H.; Velic, D.; Knoesel, E.; Hotzel, A.; Wolf, M.; Ertl, G. Dynamics of electron-induced manipulation of individual CO molecules on Cu(111). *Phys. Rev. Lett.* **1998**, *80*, 2004−2007.
(28) Fu, T.; Frommer, K.; Nuckolls, C.; Venkataraman, L. Single-molecule junction formation in break-junction measurements. *J. Phys. Chem. Lett.* **2021**, *12*, 10802−10807.
(29) Poirier, G. E. Characterization of organosulfur molecular monolayers on Au(111) using scanning tunneling microscopy. *Chem. Rev.* **1997**, *97*, 1117−1128.
(30) Tachibana, M.; Yoshizawa, K.; Ogawa, A.; Fujimoto, H.; Hoffmann, R. Sulfur-gold orbital interactions which determine the structure of alkanethiolate/Au(111) self-assembled monolayer systems. *J. Phys. Chem. B* **2002**, *106*, 12727−12736.
(31) Leary, E.; Zotti, L. A.; Miguel, D.; Márquez, I. R.; Palomino-Ruiz, L.; Cuerva, J. M.; Rubio-Bollinger, G.; González, M. T.; Agrait, N. The role of oligomeric gold-thiolate units in single-molecule junctions of thiol-anchored molecules. *J. Phys. Chem. C* **2018**, *122*, 3211−3218.

https://doi.org/10.1021/acs.jpcc.2c04370
J. Phys. Chem. C XXXX, XXX, XXX−XXX